AIAA-99-0518

CONTINUOUS WATER VAPOR MASS FLUX AND TEMPERATURE MEASUREMENTS IN A MODEL SCRAMJET COMBUSTOR USING A DIODE LASER SENSOR

B.L. Upschulte*, M.F.Miller*, M.G.Allen*
Physical Sciences Inc.
Andover, MA 01810

K. Jackson†, M. Gruber†
AFRL/PRSS
Wright-Patterson AFB, OH 45433

T.Mathur‡
Taitech, Inc.
Beavercreek, OH 45431

Abstract

A sensor for simultaneous measurements of water vapor density, temperature and velocity has been developed based on absorption techniques using room temperature diode lasers (InGaAsP) operating at 1.31 μm. Sensor calibrations of density and temperature were acquired in a laboratory hot absorption cell and on a H_2-air flat flame burner from 500 K to 2200 K. In the laboratory with 0.3 Hz bandwidth and a pathlength of 70 cm in the flame, the sensor provided a precision of better than 5% in temperature and better than 10 % in molecular density, and velocity. Optical instrumentation was developed for integrating the sensor to a model SCRAMJET combustor at the Air Force Research Laboratory Wright-Patterson AFB. Preliminary measurements in the Mach 2.1 flowfield at expanded temperatures of 540, 650, and 740 K across an 18 cm pathlength provided a temperature agreement with predictions ranging from 7 to 11%, a density agreement ranging from 17 to 56% and a velocity agreement of 25%. Measurements at higher enthalpy flow gave similar results for water density and temperature, but generated increasingly difficult beam steering influences that degraded accurate flow velocity determinations.

Introduction

Continuous measurements of in-stream data for gas dynamic and chemical processes are required for development and optimization of advanced propulsion systems. In the case of SCRAMJET engines, measurements of such data are complicated by the high enthalpy of the gas streams. Intrusive probes either do not survive or introduce unacceptable flow disturbances.[1,2] The ultimate objective is to measure the net thrust produced by the propulsion system. Especially in SCRAMJET engines, the net thrust provided by the engine is often a relatively small increase in the momentum flux (ρV^2) between large inlet and exhaust values. Thus, thrust determinations require a sensitive technique capable of simultaneous measurements of gas stream density, velocity and temperature in high enthalpy flows.

Optical sensors and diagnostics for combustion flow analysis have received considerable attention during the previous decade because of their inherently non-intrusive nature, and their ability to probe relevant species such as O_2, CO, CO_2 NO, OH, and H_2O.[3,4] Laser-based optical techniques for measurements in high enthalpy flows have undergone extensive development.[3-6] Many of the optical diagnostics have the added value of flow field mapping using planar imaging

---

*Principal Research Scientist, Member AIAA
†Aerospace Engineer
‡Research Scientist
Copyright © 1998 by Physical Sciences Inc. Published by the American Institute of Aeronautics and Astronautics, Inc. with permission.

Report Documentation Page

Form Approved
OMB No. 0704-0188

Public reporting burden for the collection of information is estimated to average 1 hour per response, including the time for reviewing instructions, searching existing data sources, gathering and maintaining the data needed, and completing and reviewing the collection of information. Send comments regarding this burden estimate or any other aspect of this collection of information, including suggestions for reducing this burden, to Washington Headquarters Services, Directorate for Information Operations and Reports, 1215 Jefferson Davis Highway, Suite 1204, Arlington VA 22202-4302. Respondents should be aware that notwithstanding any other provision of law, no person shall be subject to a penalty for failing to comply with a collection of information if it does not display a currently valid OMB control number.

1. REPORT DATE	2. REPORT TYPE	3. DATES COVERED
1998		**00-00-1998 to 00-00-1998**

4. TITLE AND SUBTITLE	5a. CONTRACT NUMBER
Continuous Water Vapor Mass Flux and Temperature Measurements in a Model Scramjet Combustor Using a Diode Laser Sensor	5b. GRANT NUMBER
	5c. PROGRAM ELEMENT NUMBER
6. AUTHOR(S)	5d. PROJECT NUMBER
	5e. TASK NUMBER
	5f. WORK UNIT NUMBER
7. PERFORMING ORGANIZATION NAME(S) AND ADDRESS(ES) **Physical Sciences Inc,20 New England Business Center,Andover,MA,01810**	8. PERFORMING ORGANIZATION REPORT NUMBER
9. SPONSORING/MONITORING AGENCY NAME(S) AND ADDRESS(ES)	10. SPONSOR/MONITOR'S ACRONYM(S)
	11. SPONSOR/MONITOR'S REPORT NUMBER(S)

12. DISTRIBUTION/AVAILABILITY STATEMENT
Approved for public release; distribution unlimited

13. SUPPLEMENTARY NOTES
The original document contains color images.

14. ABSTRACT
see report

15. SUBJECT TERMS

16. SECURITY CLASSIFICATION OF:			17. LIMITATION OF ABSTRACT	18. NUMBER OF PAGES	19a. NAME OF RESPONSIBLE PERSON
a. REPORT	b. ABSTRACT	c. THIS PAGE			
unclassified	**unclassified**	**unclassified**		**12**	

techniques[7-11] or high-speed line-of-sight absorption/ emission monitoring.[3-6, 14-21]

Diode laser absorption techniques have previously demonstrated measurements of molecular density,[14-16,21,24] temperature,[17,22-24,26] and in-stream flow velocity.[15,18,22,23] Room temperature distributed feedback (DFB) diode lasers (InGaAsP), originally developed for the communications industry, operating at 1.31 µm coincidentally overlap with weak absorption transitions of the $2\nu_3$ and $\nu_1 + \nu_3$ overtone bands of water vapor. Considering the relatively high levels of water vapor expected in combustion facilities these communications industry lasers require a serious evaluation of their capability to perform sophisticated diagnostic measurements. Advantages of these lasers include: 1) their obvious availability, 2) their excellent single mode behavior for spectroscopic measurements, i.e., bandwidth of less than 10 MHz, and current tuning ranges of more than 1.5 cm^{-1}, 3) their packaging into ruggedized fiber pigtailed mounts with butterfly electrical leads, and 4) their decreasing cost to performance ratio.

This work reports continuous simultaneous measurements of water vapor density, temperature, and velocity using room temperature distributed feedback (DFB) diode lasers (InGaAsP) operating at 1.31 µm in a model SCRAMJET combustor at the Air Force Research Laboratory Wright Patterson AFB. A stand-alone computer controlled instrument package was assembled. Two lasers were time domain multiplexed to measure selected absorption transitions of the $2\nu_3$ and $\nu_1 + \nu_3$ overtone bands of water vapor. A fiber optic network was fabricated to combine the outputs from the two diode lasers onto a dual beam launch and collection system. Below 1200 K, the sensor water temperature and density measurements were calibrated in the laboratory using a high temperature absorption cell filled with pure water vapor. Above 1200 K, the sensor temperature measurement was calibrated using a H_2-air flat flame burner equipped with a thermocouple corrected for radiation loading. Above 1200 K, the sensor water density measurement was calibrated using chemical equilibrium modeling of the conditions in the flat flame burner with known mass flows of reactants. Integration optics using water cooling and window purge gas flows were specifically developed for the field tests on the model SCRAMJET combustor at the Air Force Research Laboratory Wright Patterson AFB. Note, testing new instrumentation in practical ground based facilities is often limited due to short test times.[22-24] The model SCRAMJET combustor at the Air Force Research Laboratory at Wright Patterson AFB provides a pseudo- continuous or long duration high enthalpy flow which is well suited for testing new instrumentation.[27]

Experimental Approach

The approach for the simultaneous measurement of water vapor density, temperature and velocity using diode laser absorption techniques is shown schematically in Figure 1. Two diode lasers probing different water absorptions are propagated across the sample volume at two different angles. The lasers are frequency scanned to acquire data across the entire absorption lineshape. Each line of sight contains the two laser scans in time multiplexed mode. The resultant signals from the balanced ratiometric detector (BRD)[28-31] units are shown schematically in Figure 2.

The density of water is determined by the integrated area of any of the four absorption lineshapes and spectroscopic constants that depend only on temperature. The temperature is determined by the ratio of the integrated area of two different absorption lines. The flow velocity is determined by the relative Doppler shift in an absorption peak measured at two different angles to the flow vector. The formulas for determination of these parameters are listed below. They have been derived and described in detail previously.[17,18]

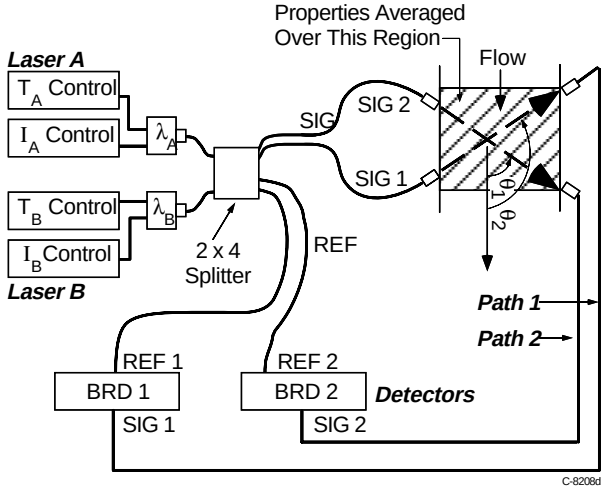

Figure 1. Schematic layout of simultaneous density, temperature and velocity measurement system.

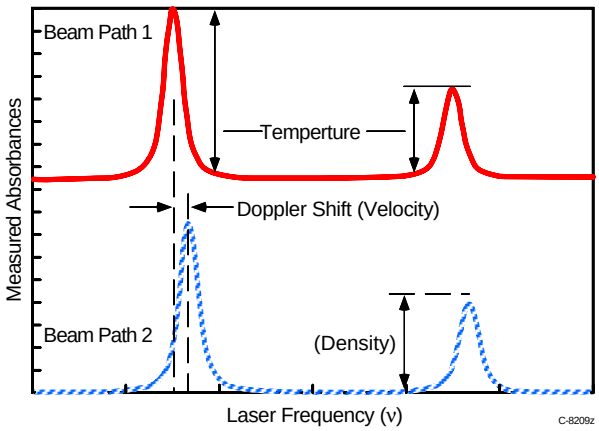

Figure 2. Signal analysis for simultaneous density, temperature and velocity measurements.

The density is determined from the formula:

$$N = \int \alpha \, d\nu/[S(T)L], \text{ and } \alpha = \ln (I_\nu / I_{\nu 0}) \qquad (1)$$

where α is the absorbance, I_ν, $I_{\nu 0}$ are the laser intensities after and before propagation through the absorbing gas, the integral is across the entire lineshape, S(T) is the linestrength of the absorption transition, and L is the pathlength.

The temperature is determined from the formula:

$$1/T = 1/T_{ref} - (k/hc\Delta E) \times \ln\left\{[\int \alpha_1 d\nu / \int \alpha_2 d\nu]/[S_1(T_{ref})/S_2(T_{ref})]\right\} \qquad (2)$$

where T_{ref} is a reference temperature, i.e., normally 298 K, k, h, c are Boltzmann's constant, Planck's constant, the speed of light respectively, the integrals are over each laser lineshape, $S_1(T_{ref})$, $S_2(T_{ref})$ are the line strength values at the reference temperature, and $\Delta E = E"_1 - E"_2$ is the energy difference between the lower state energy of each absorption transition.

The velocity is determined from the formula:

$$V = c \, \Delta\nu_{12} / [\nu_0(\cos\theta_1 - \cos\theta_2)], \qquad (3)$$

where c is the speed of light, $\Delta\nu_{12}$ is the frequency shift between the lineshapes propagated at angles θ_1, θ_2 relative to the flow vector, and ν_0 is the center frequency of the transition.

The temperature is most precisely measured using one set of absorption lines for the temperature range from 500 K to 1100 K and a second set of absorption lines for the temperature range from 1100 K to 2000 K. Analysis of the above formula shows that the temperature resolution decreases with increasing temperature, but increases with increasing separation, ΔE, in the lower state energy levels of the two transitions. Changing absorption transitions to increase the ΔE at high temperature conditions, thus allowing more precise temperature measurements. Spectroscopic parameters[32,33] of the selected transitions are presented in Table 1.

Table 1. Spectroscopic Parameters for the Selected Water Transitions

Center Frequency, ν_0 (cm^{-1})	E'' (cm^{-1})	$\nu'' - \nu'$	$\phi'' = \phi'$
Low T1			
7612.0273	285.42	000-002	3,3,0-4,4,1
7612.2682	285.42	000-002	3,3,1-4,4,0
Low T2			
7632.0931	1538.15	000-101	10,3,7-11,5,6
High T1			
7605.7967	1201.92	000-101	9,2,7-10,4,6
High T2			
7622.7a	~8821	unknown	unknown

a. Note absorption measurements on the transition at 7622.7 cm^{-1} have been analyzed to give an approximate E" level of 8821 cm^{-1}, but this transition is not assigned by either the HITRAN 98[31] or HITEMP[32] databases. Our temperature calibration in the high range was cross checked with radiation corrected thermocouple measurements.

Sensor Calibration

A significant effort was devoted to the calibration of the sensor. Low temperature calibrations were performed in a high temperature cell shown schematically in Figure 3. Line strength and collisional broadening measurements in this cell were compared with HITRAN and HITEMP predictions in a previous publication.[34]

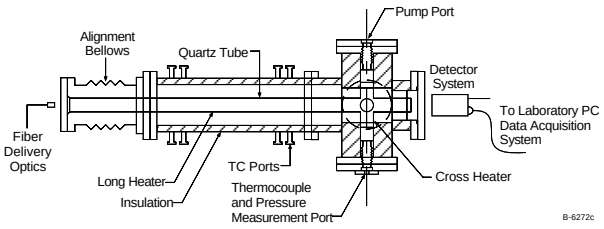

Figure 3. Schematic of high temperature absorption cell.

High temperature calibrations were performed in a well characterized[4,35] Henken-type flat flame burner. The experimental setup of the burner optics is shown schematically in Figure 4. The optics consist of f/2 spherical mirrors arranged in a Herriot geometry. An entrance slot and exit slot in the mirrors allow access for the laser beam fiber optic launch, and BRD signal detector. The mirrors are mounted on 2-D micrometers for x-y positioning , and on two-axis gimbal mounts for control of the reflection pattern and total pathlength through the flame. Calibrations were performed with a pattern of 13 reflections corresponding to 28 passes or a total in-flame pathlength of 71 cm. The total pathlength was verified by measuring the entrance and exit power of the laser and comparing to the known reflectivity of the mirrors in the IR at 1.31 µm.

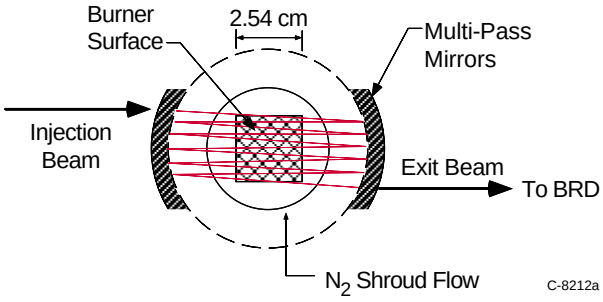

Figure 4. Schematic of optical setup around the flat flame burner.

For water density and temperature calibrations the burner was fueled with technical grade H_2 without further purification. Flows of all gases were regulated with precision needle valves and measured with MKS mass flow meters. Flows of nitrogen and oxygen in a 80:20 ratio simulated air for the burner. Nitrogen flow was metered into the shroud region of the burner to prevent entrainment of room air and water into the flow of combustion gases. Nitrogen is also metered into a purge region outside the combustion shroud to eliminate room air water absorption from the optical path, and to prevent condensation on the mirrors.

Flame measurements were preceded by simulations using a chemical equilibrium code (STANJAN) to predict water mole fractions at the flame gas temperature measured with a radiation corrected thermocouple. These predicted equilibrium mole fractions were generally within 15% of the adiabatic flame values. Measurements were performed with equivalence ratios ranging from 0.2 up to 1.0, corresponding to temperatures of 900 to 2000 K. At the lowest equivalence ratios, not all of the individual flamelets of the burner are ignited, leading to potentially larger uncertainty. An IR viewer was used to confirm ignition, flamelet stability, and overall flame shape.

A radiation corrected Pt/Pt-13% Rh thermocouple was used to measure the post combustion gas temperature. The radiation correction for the 0.010 in. bead ranged from 20 K at 1000 K to about 170 K at 2000 K.[36,37] Figure 5 presents both measured and calculated flame temperatures. Temperature profiles at several heights and across both dimensions of the flame indicated the flame profile is sharply defined with a horizontal dimension of 26 mm.

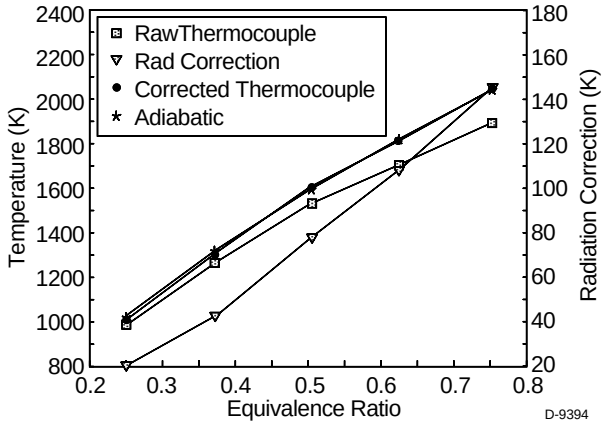

Figure 5. Flat flame burner temperature measurements and calculations.

Calibration runs on the flat flame burner involved recording both water temperature and density with the diode laser sensor simultaneous with thermocouple measurements as the equivalence ratio is changed in discrete steps. Figures 6 and 7 show the results from one calibration run. The absolute temperature accuracy is always better than 100 K, and in most cases the measurement precision is nominally ± 15 K. The absolute water density accuracy compared to STANJAN predictions is better than 6% and the precision is better

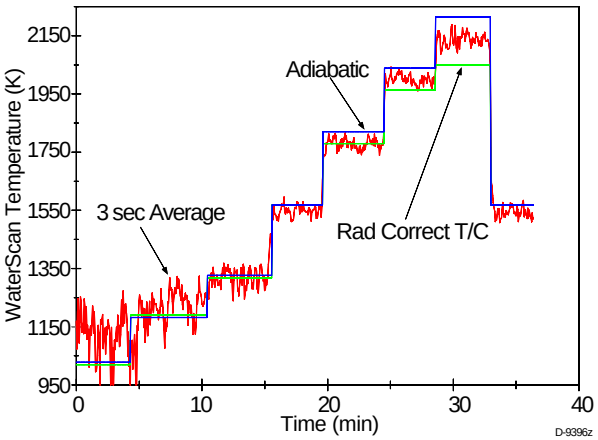

Figure 6. Temperature calibrations from thermocouple measurements and predictions of adiabatic flame temperature.

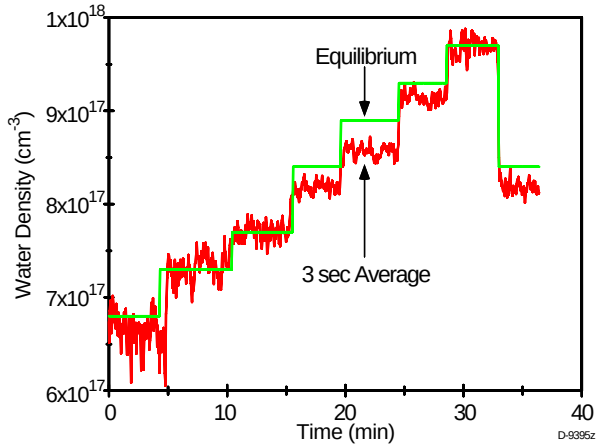

Figure 7. Water density calibration from equilibrium predictions of flat flame burner water mole fractions at atmospheric pressure.

than 1% for strongly absorbing conditions. Ancillary calibrations of laser performance, i.e., wavelength, frequency tuning, etc., have been incorporated into the temperature and density calibrations on the flat flame burner.

Sensor Engineering and Combustor Optical Hardware

The sensor has been custom engineered for the model SCRAMJET combustor at the Air Force Research Laboratory WPAFB. The sensor electronics package located in the facility control room is computer controlled and mounted in a standard half height equipment rack shown schematically in Figure 8. All laser control hardware, fiber optic splitters, data

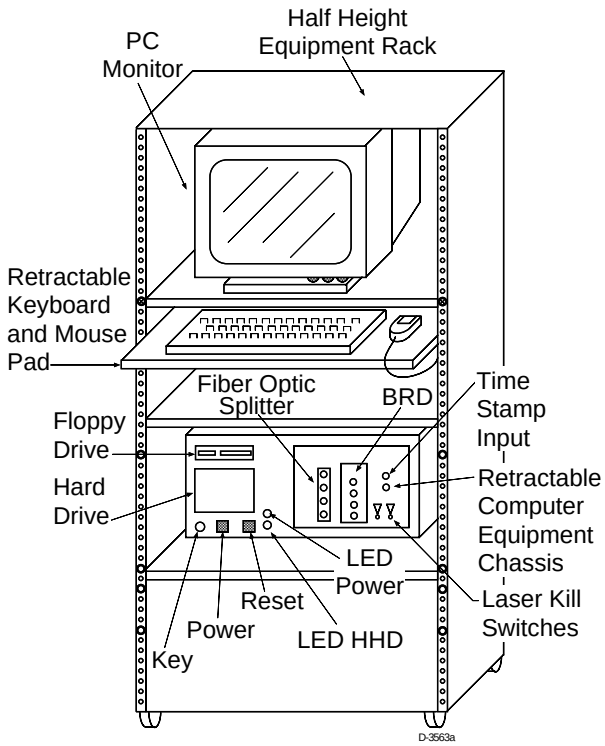

Figure 8. Schematic of sensor electronics package.

acquisition boards, etc. have been mounted within the computer chassis. An ethernet board is provided for periodic CPU clock calibration to a NIST atomic clock via internet access. System control is facilitated through keyboard and mouse interfaces to custom LabView software routines. Laser monitoring graphs and charts of temperature, density, and velocity are presented on the front panel display, and are recorded to file at user selectable rates. Fiber optic cables transport laser light to the supersonic combustion section of the model SCRAMJET, and electrical cables transport detector signals back to the computer for analysis.

Critical for high temperature applications are the design and engineering of the optical interface to the supersonic combustor. Because the steady state wall temperature of the combustor is over 400 K, it is necessary to cool the optics to protect the fiber optic collimators and InGaAs photodetectors. To achieve high absorbance sensitivity, the windows need to have anti-reflection coatings which can not survive high levels of humidity at temperatures above 500 K. In addition, particulates in the flow can become deposited on the windows, producing damage on the coatings and obscuring optical access. These considerations dictate the use of both water cooling and gaseous nitrogen film

cooling to protect the optics. Because the flowfield is supersonic, minimizing flow perturbations due to the film cooling is critical for the design.

A schematic of the film cooling system is shown in Figure 9. The IR grade fused silica windows are 1.9 cm diameter with a 2.54 cm shoulder. The windows are AR coated at 1.31 µm for an incidence angle of 15 degrees. Nitrogen is fed through machined passages in the window mount with a flow limited by a choked 2.0 mm orifice at sonic conditions. Mass flow for film cooling corresponds to about 5 scfm per window or 25 scfm total which is less than 0.5 % of the main combustor flow.

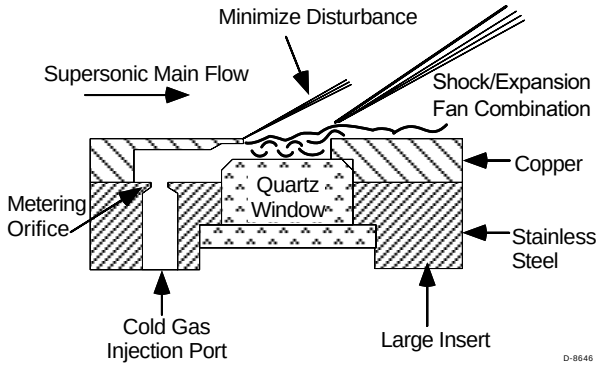

Figure 9. Schematic of gaseous nitrogen film cooling system.

Installation on the WPAFB Mach 2.1 supersonic combustion tunnel (shown schematically in Figure 10) required custom side wall panels to accommodate our optical mounts with water and gaseous cooling lines. The custom side panels, shown schematically in Figure 11, indicate connections for water cooling,

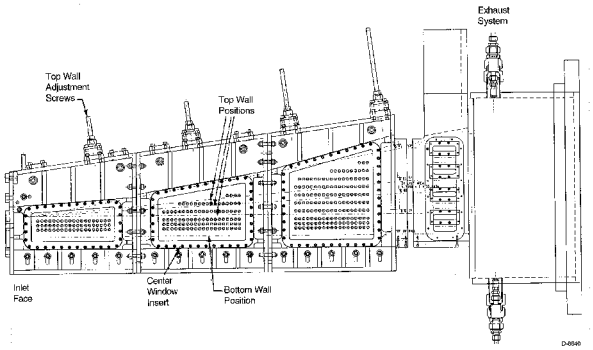

Figure 10. Supersonic Combustion tunnel at WPAFB.

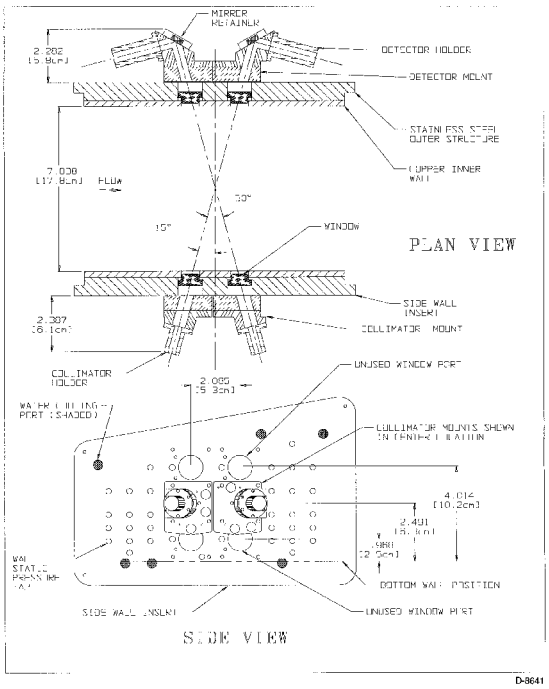

Figure 11. Water cooled side panel for optical access to WPAFB supersonic combustion tunnel.

nitrogen gas film cooling, and a variety of locations for pressure taps to monitor potential flow disturbances.

Water cooling to stabilize the panel for the optical windows requires the removal of 200 Watts of thermal power and corresponds to a 11 K temperature rise for a nominal water flow rate of 8 gallons per minute with a pressure drop of 10 psi for each panel.

Combustor Tests and Results

Preliminary tests on the model SCRAMJET supersonic combustion tunnel at WPAFB were performed without windows, fiber optics or photodetectors. Fused silica windows were replaced with steel window blanks instrumented with thermocouples. These tests were used to evaluate cooling behavior of the custom panels and to monitor the tunnel for any flow disturbances generated by the gaseous nitrogen film cooling flow. The tunnel was fitted with a nozzle to expand the freestream flow to Mach 2.1. The inlet air was heated with a SUE heater burning JP-4. The expanded static pressure could be held at either a high pressure condition of 12 psia, or a low pressure condition of 6 psia using multiple gas exhaust pumps. Stagnation

temperatures were controllably varied from 944 K to 1111 K, to 1250 K, corresponding to free stream static temperatures at the sensor line of sight location of 540, 650, and 740 K.

Tests were performed with the maximum nitrogen film cooling to evaluate potential flow disturbances. Figures 12 and 13 show wall pressure distributions with and without maximum nitrogen film cooling. No significant flow disturbances due to film cooling flow are evident in these data.

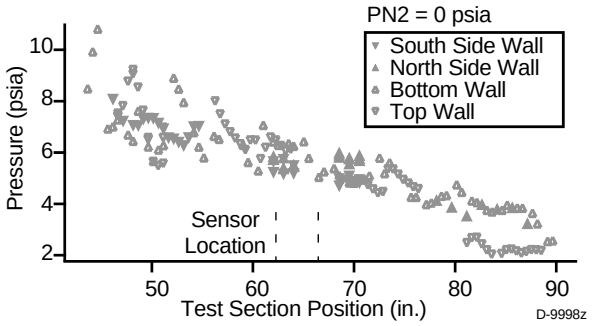

Figure 12. Pressure tap data with no gaseous nitrogen film cooling.

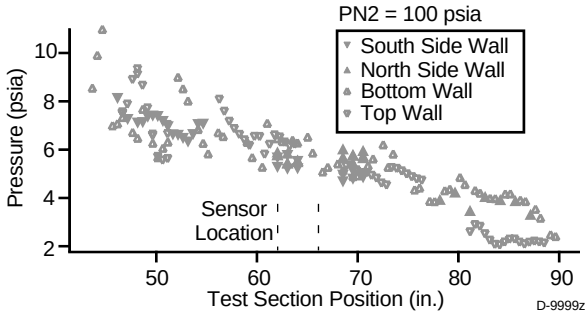

Figure 13. Pressure tap data with maximum nitrogen film cooling, shows no significant flow perturbations.

Thermocouples were monitored at several locations on the custon panel and at the steel replacement window. The maximum temperature recorded at any location on the panel or window insert was 341 K, which is well below the safe optical coating limit of 523 K. At the highest stagnation temperature, 1250 K, the water flow increased temperature by 11 K between the inlet and outlet to the custom panel. A review of the steel window inserts was performed after the test runs. The steel window inserts exhibited some contamination. The contamination was aligned with the flow direction and build up started about halfway across the steel window insert. Much of the contamination is expected to have accumulated during periods with no film cooling.

Several spectral measurements were obtained during the startup sequence and initial pump down of the tunnel. Figure 14 shows the atmospheric water absorption on the 7612 cm^{-1} doublet prior to pump down. The minimum tunnel pump down pressure is 3 psia, and the observed water absorption at the 7612 cm^{-1} doublet under these conditions is shown in Figure 15. The narrow line widths due to reduced collisional broadening are consistent with the low pressure condition.

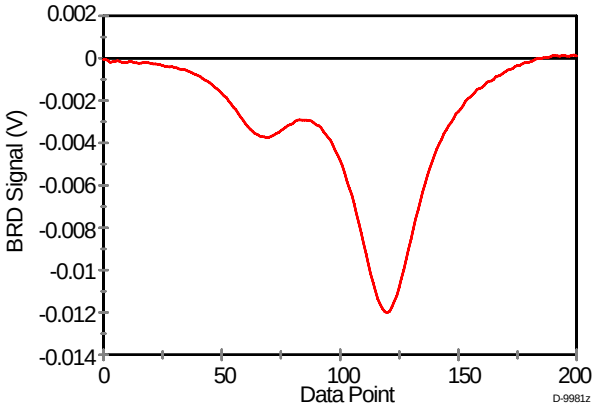

Figure 14. Room air water absorption prior to tunnel pump down.

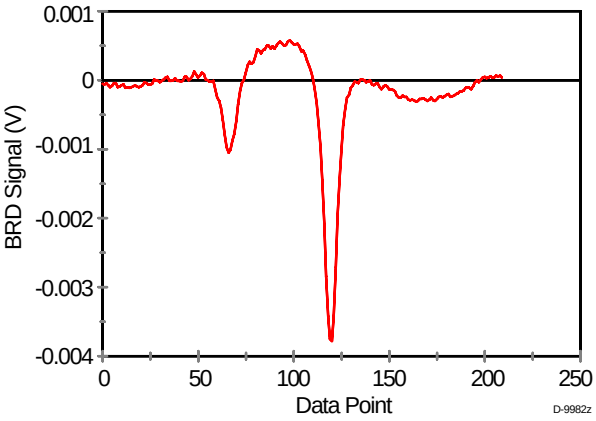

Figure 15. Water absorption lineshape at a tunnel pump down pressure of 3 psia.

Simultaneous density, temperature and velocity measurements were recorded at 1 Hz throughout a sequence of increasing stagnation temperatures 944, 1111, and 1250 K at an expanded pressure of 12 psia. Figure 16 shows the measured water density during the

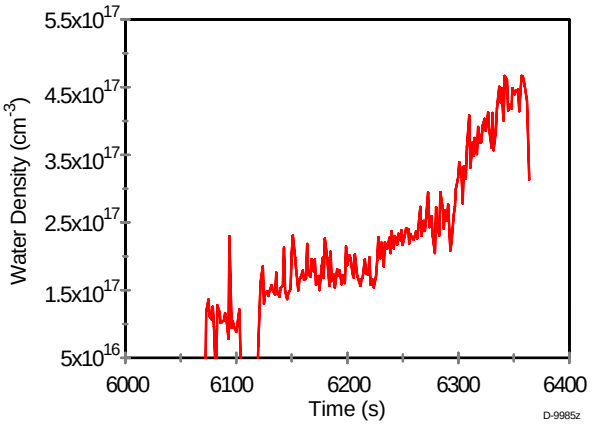

Figure 16. Water density measurements during a sequence of changing stagnation temperatures from 944 K, 1111 K, 1250 K.

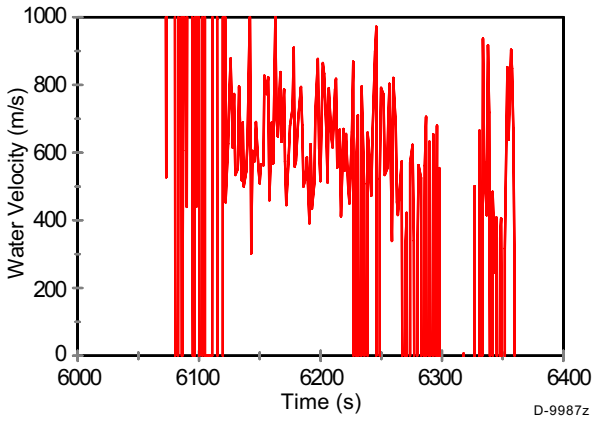

Figure 18. Simultaneous velocity measurements during a sequence of stagnation conditions, 944 K, 1111 K, 1250 K. The predicted velocities in the expanded combustor are 970, 1060, and 1130 meters/second.

sequence of changing stagnation temperatures. Figure 17 shows the simultaneous freestream static temperature measurements, and Figure 18 the simultaneous velocity measurements.

Table 2 presents a summary of the measured and predicted conditions in the expanded combustor at the sensor line of sight. Although large excursions in the sensor output were observed, the optical sensor tracks both the water density and temperature changes. The velocity measurement is the most distorted. The measured water density shows a discrepancy with predictions ranging from 17 to 56%, but has a precision of better than 10%. The measured temperatures give the best agreement with predictions, but the low signal-to-noise ratio results in temperature precisions of ± 100 K.

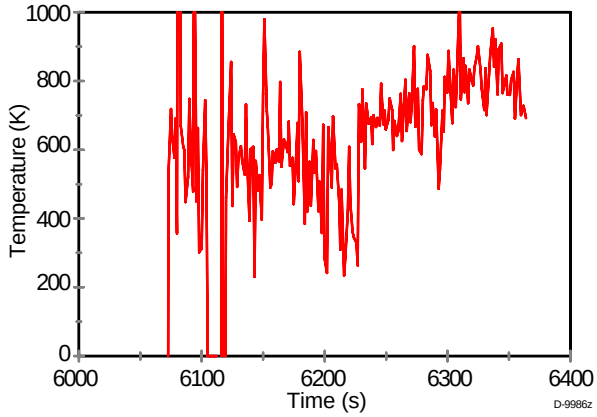

Figure 17. Simultaneous temperature measurements during a sequence of stagnation temperatures, 944 K, 1111 K, 1250 K. The predicted temperatures in the expanded combustor are 540, 650, 740 K respectively.

Analysis of the absorption lineshapes indicates several areas for improvement. Lineshapes of the two water absoprtions at time 6351 seconds, corresponding to the highest stagnation temperature, are shown in Figures 19 and 20. The signal to noise ratio in the 7612 cm^{-1} absorption is relatively good; however, the non-linear baseline, especially in the wings of the absorption, suggests potentially another absorber may be interfering with the water absorption measurement. The common combustion products CO, CO_2, OH, NO, and NO_2 are not expected to absorb in this region, but the absorption spectra of unburned JP-4 fuel and fuel fragments are not well documented at these conditions. The low signal to noise ratio in the 7632 cm^{-1} absorption line indicates a need for an absorption line with a larger line strength to improve the detection sensitivity. Table 3 presents a summary of the lineshape parameters for the absorptions observed at time 6351 seconds. The predicted and measured lineshape parameters are in relatively good agreement considering the signal-to-noise ratios in the measured lineshapes. This agreement indicates the system was operating and measuring the nominal local conditions.

The velocity measurement is the simplest calculation and yet most demanding measurement for the optical system. The sensor can obtain a density and temperature if either line of sight sees measureable absorptions. The velocity measurement requires that both lines of sight see measureable absorptions with high signal-to-noise ratios. Our current speculation is that the second line of sight was viewing through a

Table 2. Summary of Optical Measurements and Results

Condi-tion	Stagna-tion Pressure (psia)	Expanded Static Pressure (psia)	Stagna-tion Temper-ature (R/K)	Predicted[a] Expanded Static Temper-ature (K)	Measured Expanded Static Temper-ature (K)	Predicted[a] Water Fraction (%)	Measured Water Fraction (%)	Predicted[a] Flow Velocity (m/s)	Measured Flow Velocity (m/s)
1	112	12	1700/944	540 ± 20	600±100	2.5 ± 0.2	1.6 ± 10%	970 ± 25	700 ± 100
2	112	12	2000/1111	650 ± 25	700±100	3.8 ± 0.4	2.6 ± 10%	1060 ± 30	-
3	112	12	2250/1250	740 ± 30	800±100	4.8 ± 0.4	5.6 ± 10%	1130 ± 35	-

a. Data provided by test cell engineers.

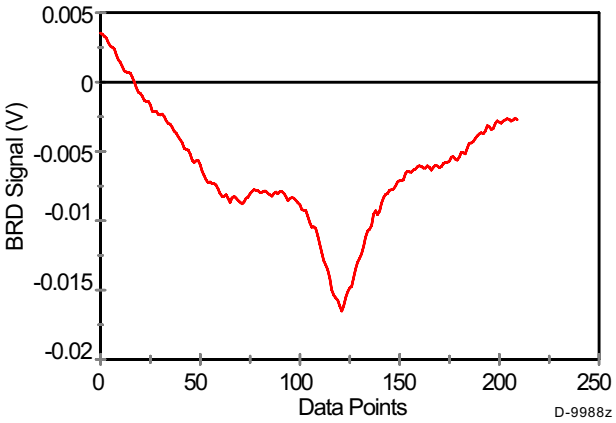

Figure 19. Lineshape of the 7612 cm^{-1} doublet at time 6351 seconds.

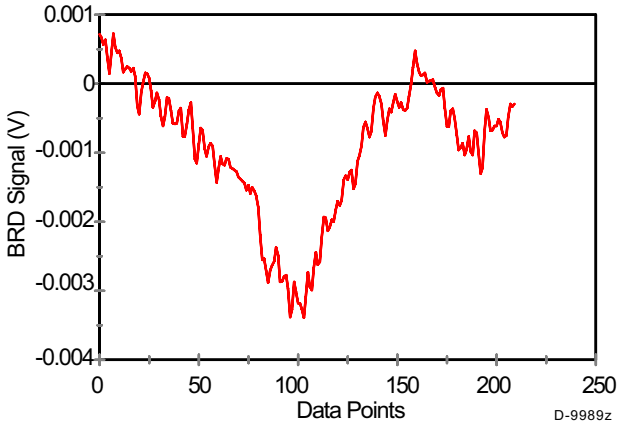

Figure 20. Lineshape of the 7632 cm^{-1} absorption at time 6351 seconds.

Table 3. Measured and Predicted Absorption Line Parameters

	Line 1[a], 7612 cm^{-1}		Line 2[a], 7632 cm^{-1}	
	Prediction	Measurement	Prediction	Measurement
α peak	1.22×10^{-3}	$(1.18 \pm 0.22) \times 10^{-3}$	6.36×10^{-4}	$(1.3 \pm 0.2) \times 10^{-3}$
$\int \alpha \, d\nu$ (cm^{-1})	2.64×10^{-4}	$(3.1 \pm 1.4) \times 10^{-4}$	1.17×10^{-4}	$(1.65 \pm 0.2) \times 10^{-4}$
$\Delta\nu$ FWHM (cm^{-1})	0.110	0.106	0.093	0.089

a. 4.8% H_2O, 740 K, 12 psia

fluctuating density gradient that caused the laser beam to deflect from the detector on the opposite side panel. This density gradient could have been self induced by the film cooling on one of the windows. Additional tests will be required to confirm this speculation.

Several suggestions arise for improving the measurement. Increasing the magnitude of the absorption would improve the signal-to-noise ratios. The selected lines may be appropriate for a H_2 fueled combustor, but appear too weak for the level of water generated by the JP-4 fueled SUE heater. The 10^3 times stronger water absorption at 7181 cm^{-1} (1.3925 μm) could be partnered to a higher E" line nearby and to enable measurements with much better signal-to-noise ratios. Larger pathlengths would serve the same

purpose but folded or multiple reflection optical path alignment produces added complications.

Summary

A sensor system using near IR diode lasers at 1.31 µm has been developed for simultaneous water density, temperature and velocity measurements in advanced aeropropulsion test facilities. The non-intrusive line of sight absorption techniques used by the sensor were extensively tested in the laboratory. High temperature absorption cell and flame studies were performed throughout the temperature range from 500 K to 2000 K. Absorption measurements were calibrated using HITRAN 98,[32] HITEMP[33] spectroscopic databases, flame chemistry modeling, and a variety of laser diagnostics. Laboratory performance with a 0.3 Hz bandwidth indicated density accuracy of better than 10%, from 10^{16} to 10^{19} cm^{-3} , a temperature accuracy of nominally 5%, from 500 K to 2000 K, and a velocity accuracy of better than 5%.

The sensor was installed on the model SCRAMJET combustor at the Air Force Research laboratory at Wright-Patterson AFB. The high temperature conditions in the combustion section of the model SCRAMJET presented a challenging optical interface. Water-cooled side panels were engineered to protect the optical components from the extreme temperatures. Window mounts were engineered with a nitrogen flow across the windows to further cool the windows and prevent contamination of the interior surfaces. Water and nitrogen flow tests on the combustor confirmed adequate cooling for the optics and verified that the nitrogen flow introduced no disturbances to the supersonic tunnel flow.

The model SCRAMJET combustor was operated with an inlet Mach number of 2.1, with stagnation conditions generated by a SUE heater burning JP-4 fuel. Experimental runs of the tunnel followed a sequence of three stagnation conditions of increasing temperature, 944 K, 1111 K, 1250 K. Conditions in the expanded region, at the sensor line of sight, were nominally 540, 650, and 740 K respectively, and could be held at a pressure of either 6 or 12 psia.

Sensor measurements in the model SCRAMJET were obtained. The sensor design parameters initially set for a H_2 fueled heater, observed much lower water concentration with a JP-4 fueled heater. Simultaneous density, temperature, and velocity measurements were obtained at the lowest temperature condition. Simultaneous density and temperature measurements were obtained at all temperature conditions. Velocity measurements were hindered by beam steering influences at the higher temperature conditions. Discrepancies with predictions were large due to the low water concentrations. The differences between measurements and predictions ranged from 17 to 56% for water density measurements, from 7 to 11% for the temperature, and nominally 25% for velocity measurements.

Supersonic combustor flow is one of the more challenging environments to probe with any type of sensor system. The current sensor demonstrated the ability to make many simultaneous non-intrusive optical measurements using near IR diode laser absorption techniques in this challenging environment. Further improvements require better matching of the absorption line strengths to the water concentration conditions. Future experiments need to verify the severity of beam steering and probe optical techniques to mitigate this influence, such as large area beams and focusing systems.

Acknowledgments

This work was supported by the Air Force Wright Laboratory under contract No. F33615-95-C-2562. We wish to thank the entire support crew at Cell #22 for their assistance during our testing at WPAFB.

References

1. Park, C., “Evaluation of Real-Gas Phenomena in High-Enthalpy Impulse Test Facilities: A Review,” *Journal of Thermophysics and Heat Transfer*, **11**(1), January-March 1997.
2. Dunn, M.G., “Experimental Study of High-Enthalpy Shock-Tunnel Flow, Part II: Nozzle-Flow Characteristics,” *AIAA Journal*, **7**, 9, Sept. 1969.
3. Upschulte, B.L., Allen, M.G., and McManus, K.R., “Fluorescence Imaging of NO, O_2 in a Spray Flame Combustor at Elevated Pressures,” Proceedings 26th Symposium (International) on Combustion, pp. 2779-2786, 1996.
4. Upschulte, B.L., Sonnenfroh, D.M., Allen, M.G., and Miller, M.F.,”In Situ, Multi-Species Combustion Sensor Using a Multi-Section Diode Laser,” Paper

No. 98-0402, AIAA 36th Aerospace Sciences Meeting, January 1998.
5. Allen, M.G., Davis, S.J., and Donohue, K., "Planar Measurements of Instantaneous Species and Temperature Distributions in Reacting Flows: A Novel Approach to Ground Testing Instrumentation," Paper No. 90-2383, AIAA 26th Joint Propulsion Conference, 1990.
6. Allen, M.G., Donohue, K., and Davis, S.J., "Species and Temperature Imaging in Liquid-Fueled Spray Flames," Paper No. 90-2440, AIAA 26th Joint Propulsion Conference, 1990.
7. Allen, M.G., Parker, T.E., Reinecke, W.G., Legner, H.H., Foutter, R.R., Rawlins, W.T., and Davis, S.J., "Fluorescence Imaging of OH and NO in a Model Supersonic Combustor, "*AIAA J.* **31**(3), p. 505, 1993.
8. Parker, T.E., Allen, M.G., Reinecke, W.G., Legner, H.H., Foutter, R.R., and Rawlins, W.T., "High Temperature Supersonic Combustor Testing with Optical Diagnostics," *AIAA J. of Prop. and Power* **9**(3), p. 486, 1993.
9. Allen, M.G., Davis, S., Kessler, W., Legner, H., McManus, K., Mulhall, P., Parker, T., and Sonnenfroh, D., "Velocity Field Imaging in Supersonic Reacting Flows Near Atmospheric Pressure, *AIAA J.* **32**(8), p. 1676, 1994.
10. Verdieck, J., Yang, T.T., Burde, D., and Allen, M., "PLIF Diagnostics for Scramjet Engine Concept Testing," Paper No. 235, 10th NASP Symposium, 1991.
11. Roberts, W.L., Allen, M.G., Howard, R.P., Wilson, G., and Trucco, R., "Measurement of Nitric Oxide in the HYPULSE Expansion Tube Facility," Paper No. 9402644, AIAA 18th Aerospace Ground Testing Conference, 1994.
12. Cassady, P.E. and Lieberg, S.F., "Planar Laser-Induced Fluorescence of NO (A-X) in Hypersonic Flowfields," Paper No. 92-2962, AIAA 23rd Plasma Dynamics and Laser Conference, 1992.
13. M. Smith, W. Williams, L. Price, and J. Jones, "Shock Tube Planar Laser-Induced Fluorescence in Support of the AEDC Impulse Facility," Paper No. 94-2649, AIAA 18th Aerospace Ground Testing Conference, 1994.
14. Sonnenfroh, D.M. and Allen, M.G., "Diode Laser Sensors for Combustor and Aeroengine Emissions Testing: Applications to CO, CO_2, OH, and NO," Paper No. 96-2226, AIAA 19th Advanced Measurement and Ground Testing Conference, June 1996.
15. Baer, D.S., Nagali, V., Furlong, E.R., Hanson, R.K., and Newfield, M.E., "Scanned- and Fixed-Wavelength Absorption Diagnostics for Combustion Measurements Using Multiplexed Diode Lasers," *AIAA J.* **34**, pp. 489-493, 1996.
16. Furlong, E.R., Baer, D.S., and Hanson, R.K., "Combustion Control Using a Multiplexed Diode-Laser Sensor System," *26th Symposium (Int) on Combustion* (Pittsburgh: The Combustion Institute, pp. 2851-2858), 1996.
17. Allen, M.G. and Kessler, W.J., "Simultaneous Water Vapor Concentration and Temperature Measurements Using 1.31 µm Diode Lasers," *AIAA J.* **34**(3), pp. 483-488, 1996.
18. Miller, M.F., Kessler, W.J., and Allen, M.G., "Diode Laser-Based Air Mass Flux Sensor for Subsonic Aeropropulsion Inlets," *Applied Optics* **35**(24), pp. 4905-4912, 1996.
19. Sonnenfroh, D.M. and Allen, M.G., "Measurements of the Second Overtone Absorption Band of NO in Ambient and Combustion Gases Using a 1.8 Micron, Room Temperature Diode Laser, "*Applied Optics* **36**, pp. 7970 - 7977, 1997.
20. Mihalcea, R.M., Baer, D.S., and Hanson, R.K., "Diode-Laser Absorption Sensor System for Combustion Monitoring and Control Applications," Paper No. 97-3356 AIAA 33rd Joint Propulsion Conference, July, 1997.
21. Kessler, W.J., Sonnenfroh, D.M., Upschulte, B.L., and Allen, M.G., "Near-IR Diode Lasers for *in-situ* Measurements of Combustor and Aeroengine Emissions," Paper No. 97-2706, 33rd AIAA Joint Propulsion Conference, July, 1997.
22. Wehe, S.D., Baer, D.S., Hanson, R.K., and Chadwick, K.M., "Measurements of Gas Temperature and Velocity in Hypervelocity Flows Using a Diode-Laser Absorption Sensor," Paper No. 98-2699, AIAA 20th Advanced Measurement and Ground Testing Technology Conference, June 1998.
23. Wehe, S.D., Baer, D.S., and Hanson, R.K., "Tunable Diode-Laser Absorption Measurements of Temperature, Velocity, and H_2O in Hypervelocity Flows," Paper No. 97-3267, 33rd AIAA/ASME/SAE/ASEE Joint Propulsion Conference, July 1997.
24. Mohamed A., Rosier, B., Henry, D., Louvet, Y., and Varghese, P.L., "Tunable Diode Laser Measurements on Nitric Oxide in a Hypersonic Wind-Tunnel," Paper No. 95-0428, AIAA 33rd Aerospace Sciences Meeting, January 1995.

25. Nagali, V., Furlong, E.R., Chou, S.I., Mihalcea, R.M., Baer, D.S, and Hanson, R.K., "Diode-Laser Sensor System for Multi-Species and Multi-Parameter Measurements in Combustion Flows," AIAA 95-2684 (1995).
26. Nagali, V., Chou, S.I., Baer, D.S., and Hanson, R.K., "Measurements of H_2O and Temperature in High Pressure Environments Using Near-IR Diode Laser Absorption," Paper No. 96-2225, AIAA 19th Advanced Measurement and Ground Testing Technology Conference, June 1996.
27. Jackson, K., Gruber, M., Mathur, T., Streby, G., Smith, C., and Billig, F., "Calibration of Newly Developed Direct-Connect High Enthalpy Supersonic Combustion Research Facility," AIAA Paper 98-1510, 8th International Space Plasmas and Hypersonic Systems and Technology Conference, April 1998.
28. Hobbs, P.C.D., "Ultrasensitive Laser Measurements Without Tears," *Appl. Opt*., 1997, **36**, 903.
29. Haller, K.L. and Hobbs, P.C.D., "Double Beam Laser Absorption Spectroscopy: Shot Noise-Limited Performance at Baseband with a Novel Electronic Noise Canceller," Quantum Spectroscopy, Proc. SPIE (1991).
30. Hobbs, P.C.D., "Shot-Noise Limited Optical Measurements at Baseband with Noisy Laser," SPIE Vol. 1376 Laser Noise, p. 216 (1990).
31. Allen, M.G., Carleton, K.L., Davis, S.J., Kessler, W.J., Otis, C.E., Palombo, D.A., and Sonnenfroh, D.M., "Ultra-Sensitive Dual-Beam Absorption and Gain Spectroscopy: Applications for Near-IR and Visible Diode Laser Sensors," *Appl. Opt*., 1995, **34**, 3240.
32. Rothman, L.S. Gamache, R.R., Tipping, R.H., Rinsland, C.P., Smith, M.A.H., Benner, D.C., Devi, V.M., Flaudt, J.-M., Camy-Peyret, A., Goldman, A., Massie, S.T., Brown, L.R., and Toth, R.A., "The HITRAN Molecular Database: Editions of 1991 and 1992," *JQSRT*, 1993, **48**, 469-507.
33. Rothman, L.S. Wattson, R.B., Gamache, R.R., Goorvetch, D., Hawkins, R.L., Selby, J.E.A., Camy-Peyret, C., Flaud, J.-M., Schroeder, J., and McCann, A., "HITEMP, the High-Temperature Molecular Spectroscopic Database," *JQSRT* (in press).
34. Upschulte, B.L. and Allen, M.G., "Diode Laser Measurements of Line Strengths and Self-Broadening Parameters of Water Vapor Between 300 and 1100 K Near 1.31 µm", *J. Quant. Spectrosc. Radiat. Transf*., **59**(6), pp. 653-670, 1998.
35. Kessler, W.J., Allen, M.G., and Davis, S.J., "Rotational Level-Dependent Collisional Broadening and Line Shift of the $A^2\Sigma^+$-$X^2\Pi$ (1,0) Band of OH in Hydrogen-Air Combustion Gases," *J. Quant. Spectrosc. Radiat. Transf.* **49(**2), p. 107, 1993.
36. Bradley D. and Entwhistle, A.G., "Determination of the Emissivity for Total Radiation of Small Diameter Platinum - 10% Rhodium Wires in the Temperature Range 600 to 1450°C," *Brit. J. Appl. Phys*, 1961, **12**, 708.
37. Grosshandler, W.L., Engle, M., and Russell, A., "Emissivity of Thermocouples for Combustion Measurements," Paper WSS/CI 80-21, Spring Meeting, Western States Section, The Combustion Institute (April 1980).